Structural Basis for the Activity and Substrate Specificity of *Erwinia chrysanthemi* L-Asparaginase[†,‡]

Khosrow Aghaiypour,[§] Alexander Wlodawer, and Jacek Lubkowski*

Macromolecular Crystallography Laboratory, National Cancer Institute at Frederick, Frederick, Maryland 21702

Received December 29, 2000; Revised Manuscript Received March 19, 2001

ABSTRACT: Bacterial L-asparaginases, enzymes that catalyze the hydrolysis of L-asparagine to aspartic acid, have been used for over 30 years as therapeutic agents in the treatment of acute childhood lymphoblastic leukemia. Other substrates of asparaginases include L-glutamine, D-asparagine, and succinic acid monoamide. In this report, we present high-resolution crystal structures of the complexes of *Erwinia chrysanthemi* L-asparaginase (ErA) with the products of such reactions that also can serve as substrates, namely L-glutamic acid (L-Glu), D-aspartic acid (D-Asp), and succinic acid (Suc). Comparison of the four independent active sites within each complex indicates unique and specific binding of the ligand molecules; the mode of binding is also similar between complexes. The lack of the α-NH_3^+ group in Suc, compared to L-Asp, does not affect the binding mode. The side chain of L-Glu, larger than that of L-Asp, causes several structural distortions in the ErA active side. The active site flexible loop (residues 15−33) does not exhibit stable conformation, resulting in suboptimal orientation of the nucleophile, Thr15. Additionally, the δ-COO^- plane of L-Glu is approximately perpendicular to the plane of $\gamma-COO^-$ in L-Asp bound to the asparaginase active site. Binding of D-Asp to the ErA active site is very distinctive compared to the other ligands, suggesting that the low activity of ErA against D-Asp could be mainly attributed to the low k_{cat} value. A comparison of the amino acid sequence and the crystal structure of ErA with those of other bacterial L-asparaginases shows that the presence of two active-site residues, $Glu63_{ErA}$ and $Ser254_{ErA}$, may correlate with significant glutaminase activity, while their substitution by Gln and Asn, respectively, may lead to minimal L-glutaminase activity.

L-Asparaginase (L-asparagine amidohydrolase, EC 3.5.1.1) is an enzyme that primarily catalyzes the conversion of L-asparagine to L-aspartic acid and ammonia. A discovery that the anti-leukemic activity of guinea pig serum is associated with its L-asparaginase activity (*1*, *2*) and isolation of this enzyme from *Escherichia coli* (*3*, *4*) brought considerable attention to bacterial L-asparaginases, leading to identification of related enzymes in several other sources. Since the early 1970s, type II *E. coli* L-asparaginase (EcA) and a related enzyme from *Erwinia chrysanthemi* (ErA) have been used as drugs in the treatment of acute childhood lymphoblastic leukemia. The basis of their clinical activity is attributed to the reduction of circulating L-asparagine in blood. Since some neoplastic cells depend on extracellular supplies of this amino acid, they are selectively killed by L-asparagine deprivation (*5*). It was shown that some of the vaccine preparations had high L-asparaginase activity and this enzyme has been used for their potency control during the production process (*6*, *7*). The therapeutic effect of vaccines used for immunotherapy of cancers such as lymphoblastic leukemia and breast cancer (*8*, *9*) was attributed to their asparaginase activity (*9*).

On the basis of their substrate specificity, bacterial L-amidohydrolases can be assigned to two major classes. The first class, represented by EcA, ErA, and *Wolinella succinogenes* (WsA) L-asparaginases, includes the enzymes that primarily utilize L-asparagine as a substrate. The enzymes belonging to the second class, also referred to as glutaminase-asparaginases, catalyze the hydrolysis of both L-asparagine and L-glutamine with comparable efficiency. The best-known examples of glutaminase-asparaginases are enzymes derived from *Pseudomonas 7A* (PGA) and *Acinetobacter glutaminasificans* (AGA). Although the anti-cancer properties were demonstrated for enzymes belonging to both classes, their practical applications were highly restricted by the side effects associated with therapy. Thus, antitumor activity of PGA demonstrated in studies with mice (*10*) was accompanied by a variety of side effects, linked (at least partially) to the L-glutaminase activity of this enzyme (*11*). L-asparaginases, with their high specificity for L-asparagine and low-to-negligible activity against L-glutamine, are reported to be less troublesome during the course of anti-cancer therapy (*12*).

Crystal structures have been reported to date for five bacterial L-asparaginases and L-glutaminase-asparaginases. For AGA and WsA, the structures corresponded to the holoenzymes (*13*, *14*), while the active sites of EcA and ErA were sometimes occupied by L-aspartic acid (*15*, *16*). Additionally, the structures of ErA and PGA with SO_4^{2-}

[†] The work of K.A. at NCI was sponsored by a short-term fellowship from the Ministry of Health and Medical Education of Iran.

[‡] X-ray coordinates and the experimental structure factors have been deposited in the Protein Data Bank (entries 1HFW and R1HFWSF, 1HG1 and R1HG1SF, and 1HG0 and R1HG0SF, for ErAG, ErAD, and ErAS, respectively).

* To whom correspondence should be addressed. Phone: (301) 846-5494. Fax: (301) 846-6128. E-mail: jacek@ncifcrf.gov.

[§] Current address: Department of Biochemistry, Tehran Medical Sciences University, Tehran, Iran.

10.1021/bi0029595 This article not subject to U.S. Copyright. Published 2001 by the American Chemical Society
Published on Web 04/19/2001

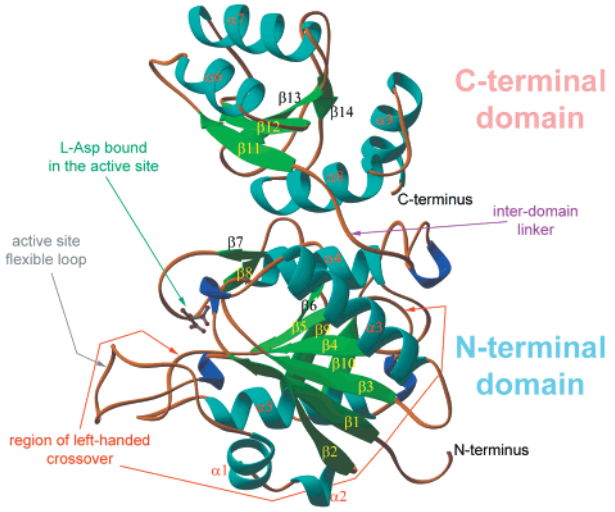

FIGURE 1: Schematic representation of the ErA monomer. Secondary structure elements in both the N-terminal (bottom) and C-terminal (top) domains are shown in different colors: α-helices in cyan, *β*-strands in green, and turns in blue. The locations of the active site and of the left-handed crossover are indicated. The molecule of L-aspartic acid, bound to the active site of the enzyme, is represented in ball-and-stick. The figure was prepared using the program Ribbons (*45*), followed by rendering with the program POV−Ray (http://www.povray.org).

located in the active site (*16*, *17*), as well as covalent complexes of PGA with 6-diazo-5-oxy-L-norleucine (DON) and with 5-diazo-4-oxo-L-norvaline (DONV) (*18*), were also published. Crystal structure of the active site mutant of EcA (T89V) was also reported (*19*) and led to the description of an acyl−enzyme intermediate. Finally, some otherwise comparable structures of L-asparaginases were solved in multiple crystal forms (*20*).

These extensive structural studies of L-asparaginases have led to detailed descriptions of their common structural features. All bacterial type II L-asparaginases are active as homo-tetramers with 222 symmetry and a molecular mass is in the range of 140−150 kDa. Each monomer consists of about 330 amino acid residues that form 14 *β* strands and eight α helices, arranged into two easily identifiable domains, the larger N-terminal domain and the smaller C-terminal domain, connected by a linker consisting of ∼20 residues (Figure 1). A crossover between the fourth and the fifth *β* strands of the N-terminal domain is left-handed (*16*). This type of a motif is rarely observed in proteins (*21*) and, when seen, is important for their activity. The left-handed crossover in L-asparaginase includes $Ala120_{ErA}$, a residue that plays an important role in the substrate/product recycling.

Each of the four active sites of L-asparaginase is located between the N- and C-terminal domains of two adjacent monomers. Their rigid cores are formed by a topological switch point (*22*) between the first and the third parallel *β* strands of the N-terminal domain and by the residues extending from the loops of the C-terminal domain of the adjacent monomer (*15*, *16*). The flexible part of the active site consists of several residues (positions 14−33 in ErA), referred to as the active site flexible loop, and covers the binding pocket upon substrate binding to the enzyme (*23*, *24*). The nucleophile, $Thr15_{ErA}$, is also located in the flexible loop region (*19*). Although each of the two intimate dimers of L-asparaginase consists of all chemical and structural elements necessary for catalysis, only tetramers of this enzyme, with four noncooperative active sites (*23*), have been observed.

Numerous studies of L-asparaginases have been conducted in order to understand the catalytic mechanism and the substrate specificity of these enzymes. Studies of the dependence of activity on pH, conducted for various L-asparaginases, confirmed that the enzymes are stable and active in the pH range of 4−9 (*25*−*27*). It has been shown that the enzymatic reaction proceeds according to a two-step ping-pong mechanism similar to the mechanism of serine proteases (*28*), except that the attacking nucleophile is a threonine. Two threonine residues, $Thr15_{ErA}$ and $Thr95_{ErA}$, are located in the active site of L-asparaginase. The crystal structure of the acyl−enzyme intermediate of $Thr89Val_{EcA}$ mutant (*19*) provided the first experimental evidence that $Thr15_{ErA}$ is the nucleophile. In their report, Röhm and Van Etten (*28*) also showed that protonated L-Asp serves as a substrate for EcA. In their isotope exchange experiments, *γ*-hydroxyl group of L-Asp is replaced by the equivalent one from a water molecule. Protonation of L-Asp is required for binding. Recently, Ortlund et al. (*18*) reported crystal structures of the covalent complexes between PGA and two suicide inhibitors, DON and DONV, further strengthening the observations by Palm et al. (*19*). The specificity toward a variety of substrates of L-asparaginases was assessed in multiple kinetic studies. Wade et al. (*29*) reported the relative activities of ErA toward L-Asn and L-Gln as 100 and 11%, respectively, and the corresponding K_m values as 0.015 and 1.4 mM. A more complete compilation of the kinetic parameters for ErA was presented by Howard and Carpenter (*30*). The relative rates of hydrolysis of L-Asn, D-Asn, L-Gln, and Suc-NH_2 by this enzyme, reported by these authors were 100, 5, 9, and 20%, respectively. Howard and Carpenter also provide the K_m (V_{max}) values for these four substrates as 0.01 mM (0.923 *μ*M/min/unit), 62 (0.177), 1.1 (0.087), 15 (0.24). Similar activities were also reported for EcA (*31*); however, L-glutaminase activity of this enzyme is much lower than for ErA.

Although the active site residues of L-asparaginases have been identified in the early crystallographic studies (*15*, *16*) and the structural as well as kinetic experiments resulted in a definition of two basic requirements for suitable active site ligand as its size (not significantly larger than that of Gln) and chemical composition, details of specificity determinants for both the enzyme and ligand molecules are just beginning to emerge. This knowledge is instrumental for providing more complete understanding of the biological properties of L-asparaginase as well as for guiding its possible modifications that would allow creation of more efficient therapeutic agents.

In this report, we describe X-ray structures of ErA complexed with L-glutamic acid, L-succinic acid, and D-aspartic acid. Throughout this report these structures will be referred to as ErAG (the complex with L-glutamate), ErAS (the complex with L-succinate), and ErAD (the complex with D-aspartate). The active sites of these newly determined structures are compared to the L-asparaginase active site occupied by L-aspartic acid (referred to as ErAL). Furthermore, a more general correlation between the structure/sequence of L-asparaginase active site and specificity of this enzyme is discussed.

Table 1: Data Processing and Refinement Statistics

	ErAS	ErAG	ErAD
temperature	room	room	liquid nitrogen
X-ray source (wavelength, Å)	rotating anode (1.5418)	rotating anode (1.5418)	synchrotron (0.98)
space group	*C*2	*C*2	*C*2
unit cell parameters			
a	107.18	108.47	105.84
b	91.32	91.70	90.43
c	128.41	130.62	126.89
β	92.04	91.94	91.80
resolution limits (Å)[a]	30.0−1.90 (1.97−1.90)	40.0−1.80 (1.86−1.80)	20.0−1.80 (1.86−1.80)
R_{symm}[b]	0.109 (0.384)	0.076 (0.337)	0.082 (0.530)
total no. of observations	228 741	270 156	331 851
no. of independent observations	91 478	102 023	100 021
completeness (%)[b]	92.4 (75.8)	86.0 (65.4)	90.1 (74.7)
avg I/σ_I[b,c]	8.3 (2.0)	7.4 (2.8)	7.4 (2.1)
refinement statistics			
no. of reflections ($>x\sigma_F$)[d]			
working set	77 804	87 857	92 573
test set	1561	1773	1881
resolution range (Å)	10.0−1.90	10.0−1.80	20.0−1.80
R-factor (free-*R*)	0.171 (0.199)	0.168 (0.188)	0.179 (0.204)
total no. of non-hydrogen atoms			
with occupancy 1.0	10 773	10 360	10 247
with occupancy 0.5	0	0	245
no. of water molecules	881	963	980
avg *B*-factor (Å^2)			
all non-hydrogen atoms	17.19	19.01	19.60
protein atoms	16.24	17.53	18.84
water molecules	27.87	33.36	27.05
rmsd from ideality			
bonds (Å)	0.005	0.006	0.005
valence angles (deg)	1.28	1.31	1.28
dihedrals (deg)	23.6	23.6	23.0
impropers (deg)	0.729	0.755	0.702

[a] Numbers in parentheses describe the high-resolution limits. [b] Values shown in parentheses correspond to the high-resolution shell. [c] *I* and σ_I describe the intensity and the standard deviation of intensity of reflection. [d] σ_F describe the standard deviation of the structure factor, while *x* equals 2 for ErAS and ErAG, and *x* equals 1 for ErAD.

MATERIALS AND METHODS

Crystallization of ErA and Preparation of Complexes. The sample of ErA used for all crystallization studies described here was a generous gift from the Intramural Research Support Program, SAIC−Frederick, where it was isolated and purified (and was used by us without further purification). All crystals used for the diffraction experiments were grown using the protocol described previously by Miller et al. (*16*). Monoclinic crystals appeared after 2−3 days and grew to their final size (deformed prisms, 0.5 × 0.5 × 0.5 mm) within a few weeks. The molecules of L-Glu, Suc, or D-Asp were bound to the active sites of the enzyme by soaking the crystals in appropriate ligand solutions. The soaking protocol consisted of four distinct steps. Initially, crystals of ErA were transferred to 35% (w/v) PEG8000 in 0.1 M Ches buffer (pH 8.5) to wash SO_4^{2-} away from the active site of the enzyme. In the second step, crystals were cross-linked with 0.1% glutaraldehyde for 1 h at 4 °C. Subsequently, cross-linked crystals were transferred to a solution containing 35% (w/v) of PEG8000 and 0.1 M sodium acetate buffer (pH 5.5). In the last step, crystals were soaked in the solution of PEG8000 and sodium acetate (identical to the previous one), containing additionally the ligand molecules at the concentrations of 0.05−0.1 M.

Data Collection and Processing, Structure Solution, and Refinement. X-ray data for ErAG and ErAS were collected from single crystals at room temperature, using a conventional radiation source. The data were recorded with a MAR Research 345 image plate detector mounted on a Rigaku RU-200 rotating-anode generator, operated at 50 kV and 100 mA. X-ray data for ErAD were collected from a single crystal at liquid nitrogen temperature. Before flash-freezing the crystal in a stream of N_2 (100 K), it was transferred to a mother liquor containing 15% glycerol. Diffraction data were collected on beamline X9B (National Synchrotron Light Source, Brookhaven National Laboratory, Upton, NY) using an ADSC Quantum 4 CCD detector. All data sets were processed and scaled using the HKL2000 suite of programs (*32*). The statistics for the three data sets are shown in Table 1.

The initial model for the refinement of all structures described here was derived from the published structure of ErA (*16*). All refinements as well as the electron density map calculations were done with the program CNS-XPLOR (*33*). For visual inspection and manual rebuilding we used the program O (*34*). In all cases, 1.5−2.0% of randomly selected experimental data were excluded from structural refinement and were used for cross-validation purposes (*35*). All water molecules and the L-aspartate bound in the active site were removed from the initial model. A rigid-body protocol was applied as the first step of refinement at the resolution of 10−2.3 Å to compensate for the differences in the unit cell parameters. Subsequently, the individual positions and *B*-factors of all non-hydrogen atoms were refined and the resolution was extended to the limits of the experimental data. Inspection of peaks in the $2F_o - F_c$ and

$F_o - F_c$ electron density maps led to the location of the water molecules and to the assignment of multiple conformations of protein residues, as well as to the introduction of the necessary corrections to the model. After several cycles of refinement, visual inspection of the electron density maps, and manual corrections, ligand molecules were placed in the enzyme active sites based on the corresponding electron density. The topology and parameter libraries for the D-Asp and Suc were generated based on those used by CNS-XPLOR for L-Asp (*36*). At the final stages, the atomic coordinates and *B*-factors were refined for the complete models of complexes, and the assessment of the geometrical and stereochemical quality of the structural models was performed with programs PROCHECK (*37*) and WHATIF (*38*). The final statistics from the structural refinement and the basic characteristics of the models are shown in Table 1.

RESULTS

Overall Structural Features of the ErA Complexes. The crystal structures of ErAG, ErAD, and ErAS were determined and refined at the resolution of 1.8 Å to 1.9 Å (Table 1). In the case of the first two structures, electron density for the active site flexible loop (a fragment spanning approximately residues 15−33 in ErA) was absent in all four monomers, indicating high mobility of this region. By contrast, the active site loops in ErAS were ordered in all four monomers, although their B-factors were elevated compared to the rest of the enzyme. The first three residues in the N-termini of the enzyme are not seen in any of the three structures due to their high mobility. The folds of the ErA molecules in all complexes are virtually identical and correspond to the previous observations (*16*) (Figure 1). Small differences in the unit cell parameters, especially when comparing ErAD to the two other complexes, are primarily attributed to different temperature during data collection. These differences are not reflected in the molecular structures since both the monomers as well as the entire tetramers of all three complexes superimpose with root-mean-square (rms) deviations of less than 0.3 Å. A majority of water molecules are structurally conserved in the three complexes, whereas multiple conformations were modeled for about 20 side chains only in the low-temperature structure (ErAD). In one of the monomers of ErAD, unexpected electron density peaks forming a toroidal shape near the NZ atom of the $Lys243_{ErA}$ were observed. The approximate radius of this density is 6.5 Å, and its plane is perpendicular to the side chain of $Lys243_{ErA}$. Since this peculiar feature was previously observed in other cryogenic structures of ErA (unpublished material), it cannot be considered an artifact. The most likely explanation of its origin is binding of a poly(ethylene glycol) molecule to the enzyme. Although specific, this interaction is rather weak, and thus observed only in the low-temperature experiments. Due to the lack of sufficiently detailed features of this electron density, we modeled it as several water molecules. It is very unlikely that this putative modification would affect enzymatic properties, although, as recently reported (*39*), L-asparaginase modified by covalent binding of poly(ethylene glycol) displays improved pharmacological properties (lower immunogenicity and higher stability in plasma).

Interactions within the Active Sites. Electron density peaks corresponding to the ligand molecules, shown in Figure 2, were very well-defined and allowed unambiguous placement and refinement of the ligands in all the active sites. Although binding of the ligand molecules to ErA was accomplished in a complicated soaking procedure, the presence of strong electron density with well-defined structural features indicates their high occupancy in the active sites of the enzyme. This high occupancy was accompanied by low average *B*-factors of the ligand atoms, comparable to or lower than the average *B*-factors of the entire protein molecules (16.0 $Å^2$ for L-Glu, 20.9 $Å^2$ for Suc, and 21.6 $Å^2$ for D-Asp), indicating relatively tight binding of these ligands to the active site of ErA. Furthermore, the specificity of binding was assessed by a structural comparison of the four independent active sites in each of the three complexes and showed that the binding mode of the ligand molecules is completely preserved in each case. The deviations between the atomic coordinates of the ligand molecules were found to be smaller than 0.15 Å, i.e., comparable to the errors of the structural determinations. The interactions between different ligands and the enzyme are shown in Figure 3. For reference, the previously reported details of the interactions between ErA and L-Asp (*16*) are also depicted (Figure 3d). The importance of the α-NH_3^+ group for binding of the ligand molecule to the L-asparaginase active site was reported in the past (*40*, *31*). We found that in the case of D-Asp, L-Glu, and L-Asp, despite the differences in the sizes and stereochemistry of these molecules, the α-NH_3^+ groups of the ligands participate in three conserved hydrogen bonds with ErA (Figure 3, panels a, b, and d). Two hydrogen bonds are formed with the carboxyl oxygen atoms of $Asp96_{ErA}$ and $Glu63_{ErA}$, respectively, whereas the third one is with a water molecule, invariantly present in all ErA active sites. The lack of α-NH_3^+ group, however, does not eliminate the binding of succinic acid to ErA. Interestingly, the water molecule usually interacting with α-NH_3^+ group of the ligand is absent in ErAS. The α-COO^- group of the ligand also interacts with the enzyme in a highly conserved fashion. One of the oxygen atoms always interacts with the amide group of $Asp96_{ErA}$ as well as with γ-OH group of $Ser62_{ErA}$. Interactions of the other oxygen atom of the ligand's α-carboxyl group and the enzyme are slightly less conserved. In the L-Asp and L-Glu, this oxygen atom forms a hydrogen bond with an amide group of $Ser62_{ErA}$, as well as another H-bond with a water molecule. Only the first of those two H-bonds is observed for the Suc molecule. However, the rearrangement of interactions for this oxygen atom is found in case of D-Asp, where the role of the $Asp96_{ErA}$(N) atom is played by the amide group of $Thr95_{ErA}$. In the case of this ligand, a hydrogen bond with a water molecule is also formed.

With the exception of L-Asp and Suc, the interactions between the side chains of the ligands and the enzyme are significantly less conserved. The networks of hydrogen bonds found for Suc and L-Asp are, as expected, nearly identical. One oxygen atom of the γ-COO^- group forms two hydrogen bonds with the main chain nitrogen atoms of $Thr15_{ErA}$ and $Thr95_{ErA}$, located on the opposite sites of the γ-carboxyl plane of the ligand, and the third forms an H-bond with a water molecule. The second oxygen atom of the γ-COO^- group in these two ligands interacts with the γ-OH group of $Thr95_{ErA}$, the main chain oxygen of $Ala120_{ErA}$, and with a

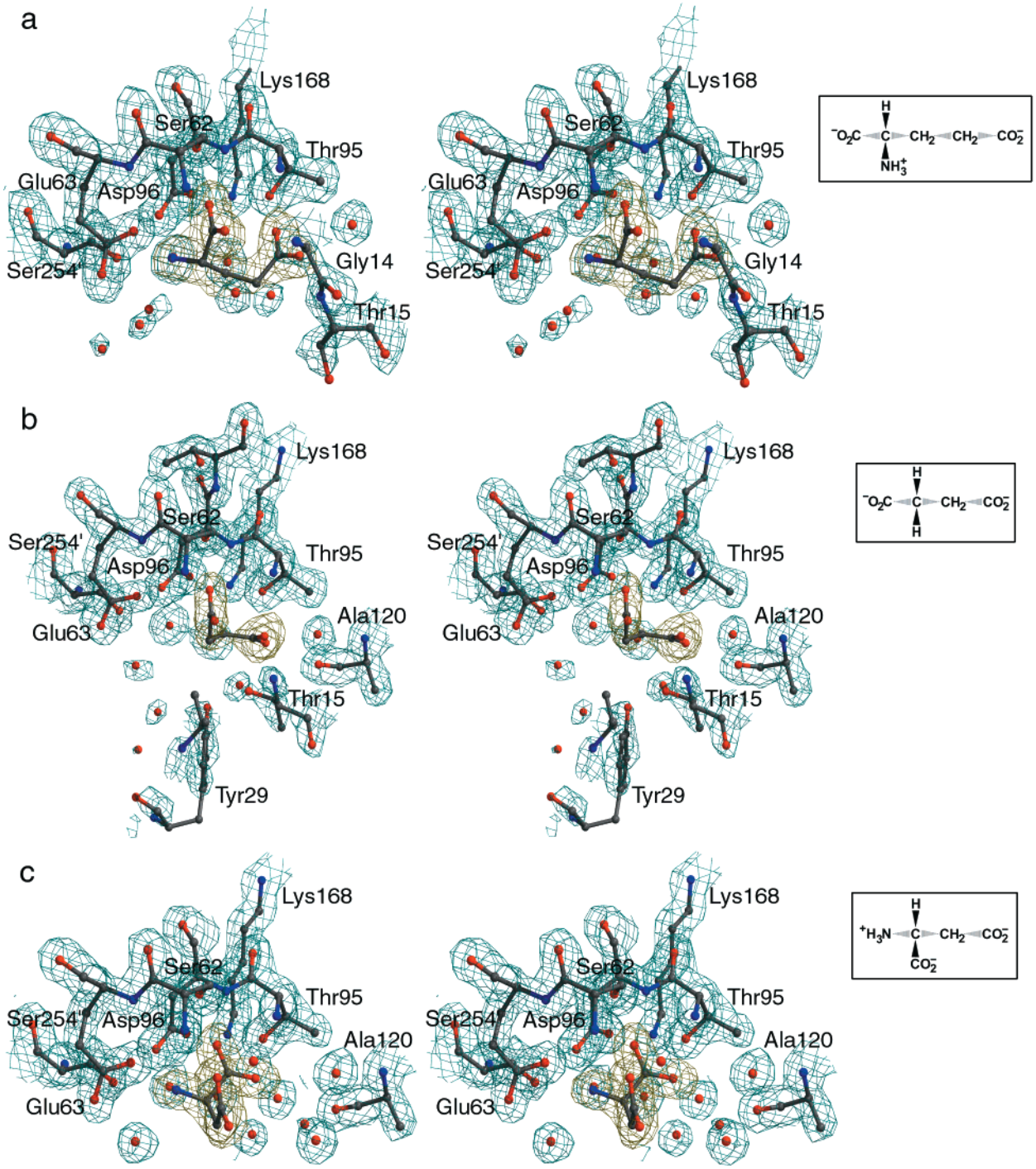

FIGURE 2: Stereo representation of the final $2F_o - F_c$ electron density maps for the active sites of three complexes of ErA. (a) The complex with L-Glu; (b) the complex with succinic acid; (c) the complex with D-Asp. Electron density maps are contoured at 1.2σ. Maps corresponding to the enzyme residues are colored in blue while maps corresponding to the ligand molecules are shown in khaki. Unlabeled spheres, shown in red, represent water molecules. These active sites are representative for each complex in terms of the structure as well as the quality of the electron density maps. This and all following figures were prepared using the program Bobscript (*46*), followed by rendering with the program POV−Ray (http://www.povray.org).

water molecule. A short contact (~3.0 Å) with the oxygen atom of $Ala120_{ErA}$ clearly indicates that the side-chain carboxyl group of the ligand is protonated.

An accommodation of the larger side chain of L-Glu in the active site of L-asparaginase is associated with two structural differences compared to the smaller L-Asp molecule. The plane of δ-COO^- group of L-Glu is nearly perpendicular to that observed for γ-COO^- group of L-Asp. Therefore, presentation of the oxygen atoms to the active site catalytic threonine residues is different. Furthermore, the bulky side chain of L-Glu prevents formation of a stable conformation of the active site flexible loop, which in this structure was found to be disordered. In the case of L-Glu, one of the side-chain oxygen atoms forms two hydrogen bonds with $Thr95_{ErA}$, one with its γ-OH group and the second with the main-chain nitrogen atom. A second oxygen atom

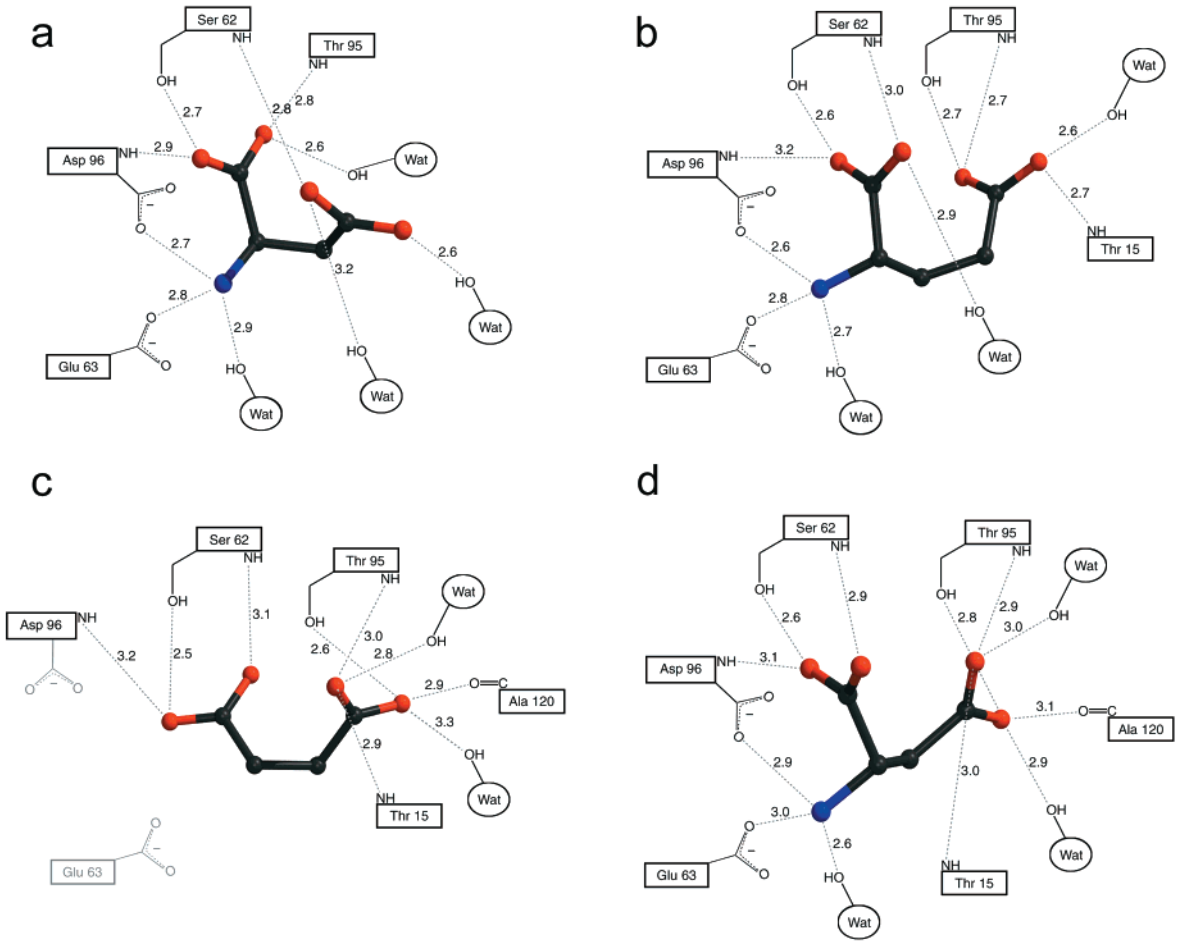

FIGURE 3: Hydrogen-bonding network between the active site atoms of ErA and the four ligands: D-Asp (a), L-Glu (b), Suc (c), and L-Asp (d). Panel d is based on the previously published structure of the complex between ErA and L-aspartic acid (*16*), kindly provided to us by Dr. Miller, and is used here for comparison. For each ligand, all of the contacts depicted in this figure are present in every one of the four active sites of ErA, i.e., water molecules that are structurally not conserved are omitted. The succinic acid molecule (c) is the only ligand lacking the α-NH_3^+ group, and consequently the interactions with the carboxyl groups of Asp96 and Glu63 are not present. However, both side chains are displayed in this panel as well (in lighter shade), due to their importance in the interactions network for other ligands.

of the side chain in this ligand also makes two hydrogen bonds, one with the main-chain nitrogen of $Thr15_{ErA}$, and the other with a water molecule. The conformation of $Thr15_{ErA}$ is different in this complex compared to the counterparts found for ErAS and the complex between ErA and L-Asp, with its side chain pointing away from the ligand molecule. Additionally, no interaction with the main chain oxygen of $Ala120_{ErA}$ was observed, and the overall number of contacts between the side chain of L-Glu and the enzyme was less than in the case of L-Asp.

A quite different situation was found for D-Asp. Its side chain points toward the active site flexible loop due to the inverted stereochemistry, preventing the formation of a stable active conformation, such as was observed for L-Asp. There are no interactions observed between the D-Asp side chain and any of the two active site threonine residues. One of the oxygen atoms of this side chain forms two hydrogen bonds with the main chain nitrogen of $Ser62_{ErA}$ and with a water molecule. The second oxygen atom interacts only with one water molecule and this interaction is conserved in all four active sites of the complex. The side chain of D-Asp forms the lowest overall number of interactions with the enzyme. As is the case for L-Glu, no hydrogen bond with $Ala120_{ErA}$ is observed.

DISCUSSION

The overall structures determined for ErAG, ErAD, and ErAS do not differ significantly from the structures of other bacterial L-asparaginases, either free or in complexes with ligands, in particular from the structures of the ErA complexed with sulfate or aspartate (*16*). Significant differences are only observed in the immediate vicinity of the active sites of the enzyme. In all the cases reported here, ligand molecules bind to all four active sites with high occupancy and in a practically identical fashion. Additionally, except for the active site flexible loop, the *B*-factors of ligand molecules are comparable with those of the surrounding protein residues.

A detailed analysis of the interactions within the active sites clearly depicts the elements determining the binding of the ligand molecules. In all cases, the α-carboxyl group of a ligand molecule and the γ-OH group of $Ser62_{ErA}$ appear to be fundamental for binding. Additionally, interactions with the main-chain nitrogen atoms of Ser62 and Asp96 indicate that the fold of the protein fragments containing these residues has to be invariant for bacterial L-asparaginases to ensure productive binding. This may be the reason behind greater rigidity of these fragments (low B-factors of con-

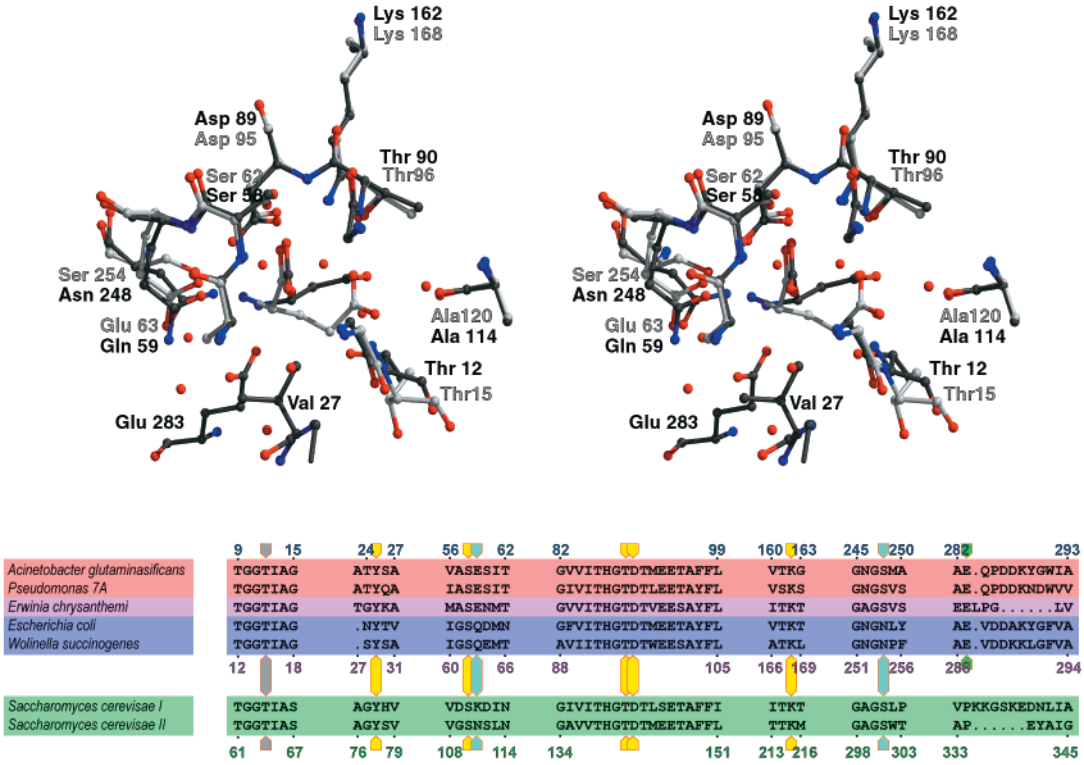

FIGURE 4: Stereo images of the active sites in the complexes of L-asparaginase, as well as the alignment of relevant amino acid sequences. The active site of the complex of ErA with L-glutamic acid (ErAG) is rendered with the light shade of the carbon atoms, while the carbon atoms in the EcA complex with L-aspartic acid (Protein Data Bank code 3ECA) are shown in darker shade. Despite very good superposition of the majority of atoms from both active sites, including parts of the ligand molecules, such differences as identities of residues at positions 63_{ErA} and 254_{ErA}, location and conformation of $Glu289_{ErA}$, and the conformation of the active site loop are found. The amino acid sequence alignment for the selected fragments of five bacterial and two yeast L-asparaginases is shown at the bottom of the figure. Sequences of bacterial enzymes with high L-Gln activity are shown on red background, the sequence of ErA (which has moderate L-Gln activity) is shown on magenta background, the sequences of two highly L-Asn specific enzymes are shown on blue background, while the sequences of yeast enzymes are shown on green background. The alignment is marked with three sets of sequence positions, one according to the EcA numbering scheme (shown at the top of alignment), the second according to the ErA numbering scheme (shown below the sequences of bacterial enzymes), and the third according to the *S. cerevisae I* (shown at the bottom of the alignment). The arrows indicate the active site residues. The position of the nucleophile is marked with gray arrow, while positions of two residues suggested here as crucial for the substrate specificity are indicated by cyan arrows.

tributing atoms) observed for all structurally studied L-asparaginases (*13*−*16*, *19*, *23*). The presence of an α-amino group in the ligand molecule undoubtfully strengthens the binding, and the side chains of two residues, $Glu63_{ErA}$ and $Asp96_{ErA}$, provide the partners needed for formation of strong hydrogen bonds. The importance of both residues was shown in mutation studies of EcA (*41*). However, formation of a complex with Suc indicates that the positive charge carried by α-NH_3^+ is not necessary for binding and processing a substrate molecule, as indicated for EcA (*40*, *31*). Although the K_m values for L-Asn and the succinic acid monoamide, 0.01 and 15 mM, respectively (*30*), show that the latter binds to ErA about 3 orders of magnitude weaker, its binding is indeed stronger than that of D-Asn, a substrate with a positively charged α-NH_3^+ group. Since there are no data showing that EcA can hydrolyze succinic acid monoamide, it is possible that the α-NH_3^+ group of a ligand molecule is a specificity determinant and that substrates lacking this feature cannot be productively bound by some bacterial L-asparaginases. Although it may appear that the role of the substrate's side chain is secondary for binding, the association of our structural results and the kinetic data, available for ErA, indicates that at least one interaction is quite significant. Such a crucial interaction is the hydrogen bond between the carboxyl group of the ligand and the main chain oxygen of $Ala120_{ErA}$. This is clearly represented by the K_m values for L-Asn and L-Gln, ~0.01 and 1.0 mM, respectively (*29*, *42*, *30*). Weaker binding is the primary reason for lower activity of ErA for L-Gln than for L-Asn, as the activity against L-Gln is only 10 times lower than this against L-Asn.

The chemical features of the ligand molecule, however, do not explain different specificities of L-asparaginases toward the two principal substrates, L-Asn and L-Gln. To gain some insight into this problem, we compared the available amino acid sequences of this enzyme from several bacterial sources as well as its two yeast variants, *Saccharomyces cerevisae* L-asparaginases I and II (ScAI and ScAII). Interestingly, we found that two residues located in close vicinity of the active site systematically differ between highly L-Asn specific L-asparaginases and the enzymes with substantial or dominating glutaminase activity (Figure 4). In all glutaminase-asparaginases, these two residues are $Glu63_{ErA}$ and $Ser254_{ErA}$, while in the highly specific L-asparaginases, they are $Gln59_{EcA}$ and $Asn248_{EcA}$, respectively (Figure 4). Simultaneous swapping of Gln to Glu and Asn to Ser affects the properties of the active site in several ways. The presence of Glu in glutaminase-asparaginases introduces an additional negative charge to the region of the active site that forms the framework for substrate binding, increasing the interactions with the positively charged α-amino group of the

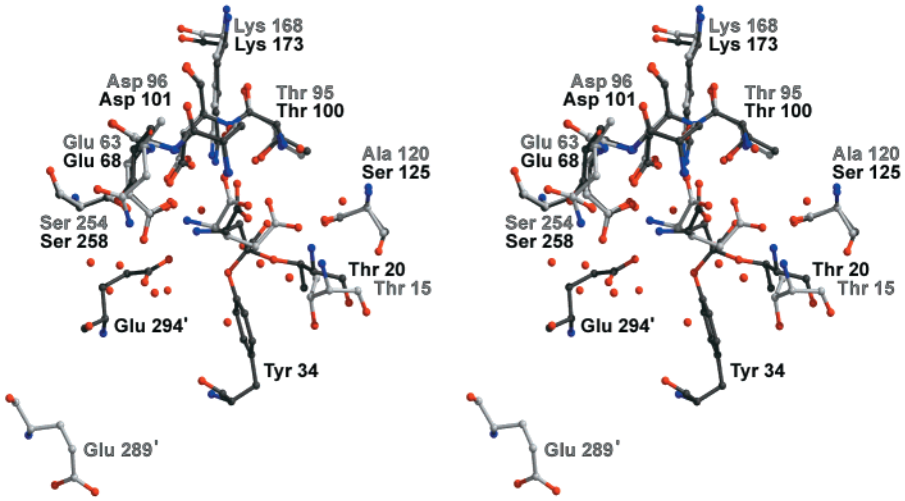

FIGURE 5: Stereo representation of the active sites of the complex between ErA and L-Glu (shown in lighter shade) and the covalent complex between PGA and DON, based on the Protein Data Bank entry 1DJP (*18*). A dramatically different location and orientation of the two equivalent glutamate residues, $Glu289'_{ErA}$ and $Glu294'_{PGA}$, and the lack of interactions between this residue and the active site Tyr29 in ErA (not visible in this structure), may raise a question regarding its postulated role in the activation of the nucleophile, $Thr15_{ErA}$.

substrate. Such substitution, however, brings two negatively charged residues, $Asp96_{ErA}$ and $Glu63_{ErA}$, close to each other. Moreover, in enzymes with high L-glutaminase activity, such as AGA and PGA, the change of Gln to Glu leads to a concentration of three negatively charged side chains, $Asp101_{PGA}$, $Glu68_{PGA}$, and $Glu294_{PGA}$. The constellation of negatively charged side chains is, however, consequently stabilized by the second substitution, of $Asn248_{EcA}$ by $Ser254_{ErA}$. The γ-OH group of the serine residue not only intercepts direct interaction between $Asp96_{ErA}$ and $Glu63_{ErA}$, forming hydrogen bonds with both side chains, but also increases the size of the active side pocket compared to the more bulky asparagine side chain in highly L-Asn specific enzymes.

In the complexes of ErA with L-Glu, the ligand molecule is slightly shifted (by ~0.5 Å) toward $Ser254_{ErA}$ compared to L-Asp (Figure 4). A similar shift could not be accommodated in the active site of EcA without conformational changes of the $Asn248_{EcA}$ side chain, which is involved in forming a network of strong hydrogen bonds. Additionally, we find that the L-glutaminase activity of ErA is relatively low compared to AGA or PGA. In the latter two enzymes, the activity toward L-Gln equals or even exceeds the activity toward L-Asn, and we suggest two factors as being responsible. One, already mentioned above, is the concentration of three negatively charged side chains around the α-NH_3^+ group of the substrate (as compared to two in ErA), introducing strong interactions that compensate for its larger size. The second factor is likely associated with the conformation of the substrate's side chain, as will be shown below. The importance of both $Glu63_{ErA}$ and $Ser254_{ErA}$ appears to extend also over the two yeast enzymes, ScAI and ScAII, that lack L-glutaminase activity. Although a serine is found in both yeast enzymes in the location equivalent to $Ser254_{ErA}$, the position equivalent to $Glu63_{ErA}$ is represented by either a lysine (ScAI) or an asparagine (ScAII), i.e., residues that do not introduce additional negative charges to the active site and, therefore, do not require stabilization by $Ser254_{ErA}$. In fact, one might suspect that $Lys111_{ScAI}$ could form a salt bridge with $Asp142_{ScAI}$ (the residue equivalent to $Asp96_{ErA}$), neutralizing its negative charge. Moreover, in both yeast enzymes the position equivalent to $Glu294_{PGA}$ contains a proline (Figure 4), consequently lacking also the negative charge contributed by this residue in AGA and PGA. Recently, Derst et al. (*43*) described the importance of $Asn248_{EcA}$ for the L-glutaminase specificity of EcA. Although the activity toward L-glutamine is reduced compared to the wild-type EcA for all mutants studied by them [Asn → (Ala, Gly, Asp, Gln, Glu)], it does not contradict our observations, as the negative charge provided by $Glu63_{ErA}$ is absent. Additionally, even the double mutation of appropriate residues of EcA would likely require the presence of a serine or a threonine in position 248 of this enzyme.

Despite correlating the structural features of the active site of L-asparaginases and the binding specificity for different substrates, conformational analysis of substrate molecules provides better understanding of the differences in catalytic process (as expressed by the k_{cat} or V_{max} values from kinetic experiments). As expected, the simplest picture is found for Suc, which binds to the active site in nearly identical mode to that observed for L-Asp (*16*). Howard and Carpenter (*30*) showed that both substrates are hydrolyzed with comparable rates (as expressed by similar V_{max} values). However, significantly lower rates of hydrolysis of L-Gln and D-Asn compared to L-Asn are direct consequences of the orientation of their side-chain amide groups toward the nucleophile, $Thr15_{ErA}$. As already discussed, binding of either L-Glu or D-Asp prevents the stabilization of the active site flexible loop in its active conformation, leading to unfavorable positioning of the side chain of $Thr15_{ErA}$. Additionally, $Tyr29_{ErA}$, important for the enzymatic activity (*24*), is completely disordered. Clearly, for nucleophilic attack to take place, the active site flexible loop (or at least its fragments containing $Thr15_{ErA}$ and $Tyr29_{ErA}$), as well as the side chains of the ligands, have to assume conformations in which γ-OH of $Thr15_{ErA}$, assisted by ζ-OH group of Tyr 29_{ErA}, and the hydrolyzed amino group of the substrate are in the locations and orientations supporting such an attack. In contrast to L-Asn and the succinic acid monoamide, where such conformations are achieved and stabilized upon binding, they are likely to be only transient for L-Gln and D-Asn, thus decreasing the likelihood of nucleophilic attack. However,

it needs to be noted that this decreased probability limits only the initial stage of catalysis, since, following the nucleophilic attack, suitable conformations of the reacting moieties are preserved by covalent binding of the substrate molecule. An additional question again arises of why, in the case of glutaminases-asparaginases such as PGA and AGA, is the glutaminase activity comparable to the asparaginase activity. A possible explanation of this feature points to the interaction of the substrate molecule with $Ala120_{ErA}$. As shown in Figures 2b, 4, panels c and d, and 5, a hydrogen bond with $Ala120_{ErA}$ stabilized the substrate in a conformation favorable for catalysis. It was previously reported (*28*) that the product of catalysis, L-Asp, can also act as a substrate for L-asparaginase, and as shown in a number of structural studies (*15*, *16*), protonated L-Asp and succinic acid bind readily to the enzyme's active site. It was postulated (*16*) that this interaction is responsible for product release, since the hydrogen bond between the amide group of the substrate is converted to a repulsive interaction between the charged carboxyl group of the product and the main-chain oxygen atom of $Ala120_{ErA}$. However, in terms of these reports, it is evident that the product may inhibit the hydrolysis of a substrate, especially at lower pH when it is stabilized in the active site. In the case of L-Gln and D-Asn, on the other hand, we do not observe any stabilization of the ligand molecule by $Ala120_{ErA}$; therefore, any inhibition of hydrolysis by the product of the catalytic reaction would be insignificant. This leads to a possibility that the gain in affinity caused by the presence of three negatively charged side chains in glutaminase-asparaginases, surrounding the α-amino group of the substrate, compensates for the lack of substrate stabilization by the $Ala120_{ErA}$, yet does not interfere with the release of the product.

Recently, Ortlund et al. (*18*) reported structural studies of covalent complexes between PGA and its suicide inhibitors, DON and DONV. In their report, they confirmed the previous observation of Palm et al. (*19*) that the $Thr20_{PGA}$ should serve as the nucleophile and additionally suggested a fundamental role of $Tyr34_{PGA}$ and $Glu294_{PGA}$ for catalysis. Their model for the activation of γ-OH group of $Thr20_{PGA}$ by the negative charge of δ-COO^- group of $Glu294_{PGA}$ requires a direct interaction between $Glu294_{PGA}(COO^-)$ and $Tyr34_{PGA}(OH)$. As shown in Figure 5, the superposition of the active sites of the complexes PGA-DON and ErAG shows significant differences between these enzymes. The overall misalignment of the highly homologous ligand molecules is the result of the considerations described above. It should be kept in mind that L-Glu represents the substrate bound prior to the catalytic reaction, while DON describes the intermediate after the nucleophilic attact, repositioned and restrained by covalent linkage to the enzyme. Although the lack of superposition of the equivalent active site Tyr residues in both structures is a direct result of the disorder in ErAG, a strikingly different location and orientation of $Glu289_{ErA}$ compared to the equivalent $Glu294_{PGA}$ results directly from the differences in the length of amino acid sequences of both enzymes in the corresponding regions. Additionally, the structure of ErA in the region containing $Glu289_{ErA}$ is conserved among all complexes of this enzyme, including those with the well-ordered active site flexible loop [L-Asp and SO_4^{2-} (*16*) and Suc]. Therefore, without significant structural changes of the residues $Ser287_{ErA}$ through $Gly292_{ErA}$, the carboxyl group of $Glu289_{ErA}$ cannot be located in direct contact with the hydroxyl group of the active site tyrosine. The results of kinetic studies of EcA with $Glu283_{EcA}$ mutated to Gln (*41*, *44*) suggest that this residue is important for binding of L-asparagine, yet secondary for catalysis.

It is worth mentioning that ErA is the only one among all reported bacterial L-asparaginases with a different length of the peptide chain in the region of $Glu289_{ErA}$. To better understand the possible consequences of this difference, we are currently conducting structural studies of the complexes of ErA with the inhibitors that were previously described in the context of their interactions with PGA (*18*).

ACKNOWLEDGMENT

We thank Dr. Z. Dauter for the help in data collection on beamline X9B (NSLS) and Dr. S. Cater for editorial comments.

REFERENCES

1. Broome, J. D. (1961) *Nature 191*, 1114−1115.
2. Broome, J. D. (1968) *Br. J. Cancer 22*, 595−602.
3. Mashburn, L. T., and Wriston, J. C. (1964) *Arch. Biochem. Biophys. 105*, 450−452.
4. Roberts, J., Prager, M. D., and Bachynsky, N. (1966) *Cancer Res. 26*, 2213−2217.
5. Haley, E. E., Fisher, G. A., and Welch, D. A. (1961) *Cancer Res. 21*, 532−536.
6. Beumer-Jachmans, M. P. (1973) *Ann. Microbiol. 124*, 289−292.
7. Soru, E., and Zaharia, O. (1974) *Immunochemistry 11*, 791−795.
8. Hortobagyi, G. N., Yap, H. Y., Wiseman, C. L., Blumenschein, G. R., Buzdar, A. U., Legha, S. S., Gutterman, J. U., Hersh, E. M., and Bodey, G. P. (1980) *Cancer Treat. Rep. 64*, 157−159.
9. Stryckmans, P. A., Otten, J., Delbeke, M. J., Suciu, S., Fiere, D., Bury, J., Solbu, G., and Benoit, Y. (1983) *Blood 62*, 606−615.
10. Roberts, J., Schmid, F. A., and Rosenfeld, H. J. (1979) *Cancer Treat. Rep. 63*, 1045−1054.
11. Wu, M. C., Arimura, G. K., and Yunis, A. A. (1978) *Int. J. Cancer 22*, 728−733.
12. Distasio, J. A., Salazar, A. M., Nadji, M., and Durden, D. L. (1982) *Int. J. Cancer 30*, 343−347.
13. Lubkowski, J., Wlodawer, A., Housset, D., Weber, I. T., Ammon, H. L., Murphy, K. C., and Swain, A. L. (1994) *Acta Crystallogr., Sect. D 50*, 826−832.
14. Lubkowski, J., Palm, G. J., Gilliland, G. L., Derst, C., Röhm, K. H., and Wlodawer, A. (1996) *Eur. J. Biochem. 241*, 201−207.
15. Swain, A. L., Jaskólski, M., Housset, D., Rao, J. K. M., and Wlodawer, A. (1993) *Proc. Natl. Acad. Sci. U.S.A. 90*, 1474−1478.
16. Miller, M., Rao, J. K. M., Wlodawer, A., and Gribskov, M. R. (1993) *FEBS Lett. 328*, 275−279.
17. Jakob, C. G., Lewinski, K., LaCount, M. W., Roberts, J., and Lebioda, L. (1997) *Biochemistry 36*, 923−931.
18. Ortlund, E., LaCount, M. W., Lewinski, K., and Lebioda, L. (2000) *Biochemistry 39*, 1199−1204.
19. Palm, G. J., Lubkowski, J., Derst, C., Schleper, S., Röhm, K. H., and Wlodawer, A. (1996) *FEBS Lett. 390*, 211−216.
20. Jaskólski, M., Kozak, M., Lubkowski, J., Palm, G., and Wlodawer, A. (2001) *Acta Crystallogr., Sect. D57*, 369−377.
21. Richardson, J. S. (1981) *Advances in Protein Chemistry*, pp 167−339, Academic Press, New York.
22. Branden, C., and Tooze, J. (1991) *Introduction to Protein Structure*, Garland Publishing, New York.
23. Lubkowski, J., Wlodawer, A., Ammon, H. L., Copeland, T. D., and Swain, A. L. (1994) *Biochemistry 33*, 10257−10265.

24. Aung, H. P., Bocola, M., Schleper, S., and Röhm, K.-H. (2000) *Biochim. Biophys. Acta 1481*, 349−359.
25. Wehner, A., Harms, E., Jennings, M. P., Beacham, I. R., Derst, C., Bast, P., and Röhm, K. H. (1992) *Eur. J. Biochem. 208*, 475−480.
26. Distasio, J. A., Niederman, R. A., Kafkewitz, D., and Goodman, D. (1976) *J. Biol. Chem. 251*, 6929−6933.
27. Roberts, J., Holcenberg, J. S., and Dolowy, W. C. (1972) *J. Biol. Chem. 247*, 84−90.
28. Röhm, K. H., and Van Etten, R. L. (1986) *Arch. Biochem. Biophys. 244*, 128−136.
29. Wade, H. E., Elsworth, R., Herbert, D., Keppie, J., and Sargeant, K. (1968) *Lancet 2*, 776−777.
30. Howard, J. B., and Carpenter, F. H. (1972) *J. Biol. Chem. 247*, 1020−1030.
31. Röhm, K. H., and Schneider, F. (1971) *Hoppe Seyler's Z. Physiol. Chem. 352*, 1739−1743.
32. Otwinowski, Z., and Minor, W. (1997) *Methods Enzymol. 276*, 307−326.
33. Brünger, A. T., Adams, P. D., Clore, G. M., DeLano, W. L., Gros, P., Grosse-Kunstleve, R. W., Jiang, J. S., Kuszewski, J., Nilges, M., Pannu, N. S., Read, R. J., Rice, L. M., Simonson, T., and Warren, G. L. (1998) *Acta Crystallogr., Sect. D 54*, 905−921.
34. Jones, T. A., and Kieldgaard, M. (1997) *Methods Enzymol. 277*, 173−208.
35. Brünger, A. T. (1992) *Nature 355*, 472−474.
36. Engh, R., and Huber, R. (1991) *Acta Crystallogr., Sect. A47*, 392−400.
37. Laskowski, R. A., MacArthur, M. W., Moss, D. S., and Thornton, J. M. (1993) *J. Appl. Crystallogr. 26*, 283−291.
38. Vriend, G. (1990) *J. Mol. Graphics 8*, 52−56.
39. Asselin, B. L. (1999) *Adv. Exp. Med. Biol. 457*, 621−629.
40. Herrmann, V., Röhm, K. H., and Schneider, F. (1974) *FEBS Lett. 39*, 214−217.
41. Wehner, A. (1993) Ph.D. Thesis, Philipps-Universität, Marburg, Germany.
42. Wade, H. E. (1977) *Dev. Biol. Stand. 38*, 73−79.
43. Derst, C., Henseling, J., and Röhm, K. H. (2000) *Protein Sci. 9*, 2009−2017.
44. Schleper, S. (1999) Ph.D. Thesis, Philipps-Universität, Marburg, Germany.
45. Carson, M. (1991) *J. Appl. Crystallogr. 24*, 958−961.
46. Esnouf, R. M. (1999) *Acta Crystallogr., Sect. D 55*, 938−940.

BI0029595